Growth and characterization of the chalcopyrite LiGaTe$_2$: A highly non-linear birefringent optical crystal for the mid-infrared

V. Petrov [a,*], L. Isaenko [b], A. Yelisseyev [b], P. Krinitsin [b], V. Vedenyapin [b], A. Merkulov [b], J.-J. Zondy [c]

[a] *Max-Born-Institute for Nonlinear Optics and Ultrafast Spectroscopy, 2A Max-Born-Str., D-12489 Berlin, Germany*
[b] *Branch of Institute of Mineralogy and Petrography, SB RAS, 43 Russkaya Str., 630058 Novosibirsk, Russia*
[c] *Institut National de Métrologie, Conservatoire National des Arts et Métiers, 292 rue Saint-Martin, F-75003, Paris, France*

Available online 23 May 2006

Abstract

LiGaTe$_2$ crystals have been grown by the Bridgman–Stockbarger technique. The clear transparency range of LiGaTe$_2$ extends from 2.5 to 12 μm and its band-gap at room temperature is at 2.41 eV (515 nm). LiGaTe$_2$ is a positive uniaxial crystal which possesses sufficient birefringence for phase-matching. Its non-linear coefficient d_{36} estimated by phase-matched second harmonic generation is 43 pm/V ± 10% at 4.5 μm. The properties of LiGaTe$_2$ are compared to those of other mid-IR chalcopyrite non-linear optical crystals with special emphasis on the frequency doubling potential for CO$_2$ lasers operating at 10.6 μm.
© 2006 Elsevier B.V. All rights reserved.

1. Introduction

The first LiGaTe$_2$ (LGT) crystals grown in 1997 by the Tammann–Stöber technique were black in color and did not exhibit a single phase, decomposing within hours into small-grained mixtures of LGT, GaTe and Te [1]. Nevertheless, from powder X-ray diffraction it was possible to confirm the chalcopyrite (CuFeS$_2$) structure (non-centrosymmetric space group $I\bar{4}2d$ or D_{2d}^{12}, Nr.122) of LGT and measure the lattice constants [1]. It was only recently that the Bridgman–Stockbarger technique was successfully applied for the growth of LGT [2]. Here we review the studied linear and non-linear optical properties of LGT, evaluate its place among the other mid-IR non-linear crystals, and speculate about some potential applications.

2. Crystal growth, transparency and band-gap of LGT

Crystals of LGT were grown by the Bridgman–Stockbarger technique in a vertical two-zone furnace with a diaphragm. The composition of the starting charge differed from the stoichiometric one to account for the incongruent evaporation near the melting temperature connected with Li and Te loss and the high chemical reactivity of Li-containing components and their interaction with the container walls. The obtained polycrystalline charge was loaded into a ampoule with several layers of pyrolitic graphite deposited on its inner surface. The free space was filled with purified Ar. The ampoule with the melted content was shifted to the cold zone with a rate of 2–5 mm/day and typical axial temperature gradients were 2–4 °C/mm. More details on the growth procedure can be found in [3,4]. We established that the deviation from stoichiometry in the melt is an important parameter that determines to a great extent the quality of the resulting crystals.

The as grown or cleaved LGT crystals (maximum sizes of about 0.5 cm^3) have natural faces of complex shape and different color depending on the thickness: from yellow for thin pieces to red and even black for thicker ones (Fig. 1). The variation of the LGT color from yellow to black (opaque for visible light) is a result of composition deviation from stoichiometry and the presence of native point defects in the bulk or the near surface layer in the case of polishing. The smooth transmission variation at shorter wavelength is indicative of light scattering or inclusions of side phases (Fig. 2). As in the case of other multicomponent chalcogenides, an additional high temperature annealing in special atmosphere is expected to improve the transparency in this spectral region.

We established that even thin samples change their color to black after polishing which deteriorates the transmission. There is also some aging of the polished surfaces which reduces the overall transmission within days. While repolishing can restore the maximum transmission, the residual absorption, especially in the near-IR, remains unchanged (Fig. 2). Unfortunately, we have still not identified the chemical process responsible for changing the properties of the surface layer. Thus, the transparency window of the now available LGT crystals depends on the absorption level assumed and the sample surface (Table 1).

It can be seen from Fig. 2 that LGT transmits up to 16 μm but the clear transparency region for as grown yellow crystals actually extends from 2.5 to 12 μm. Even for yellow crystals residual absorption (or scattering) is still present at shorter wavelengths close to the band-gap. The band-gap itself is rather large for a mid-IR crystal. For more precise estimation of it we used a thin (≈250 μm) yellow plate of LGT with natural faces. The fundamental absorption edge was measured at 11 different temperatures from 80 K to 325 K (Fig. 3). It corresponds to direct allowed electronic transitions. The band-gap is 2.41 eV
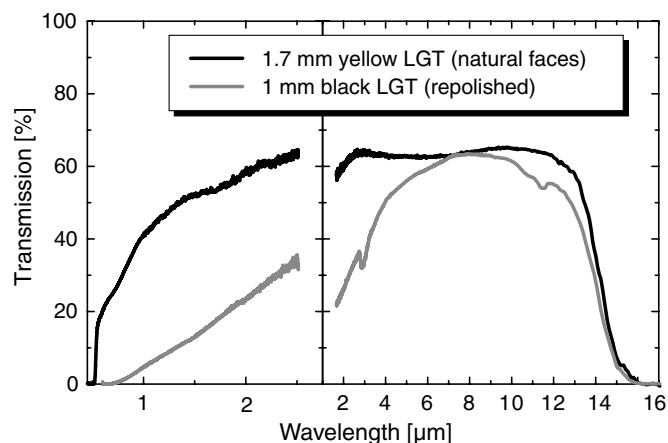
Fig. 2. Unpolarized transmission of a 1.7 mm thick plate of yellow as grown LGT with natural faces (black lines) and appr. 1 mm thick polished black plate of LGT which was stored for 3 months and then repolished (gray lines).

Table 1
Transparency of yellow and black (repolished) LGT at different absorption levels

Absorption level	3 cm^{-1}	5 cm^{-1}	10 cm^{-1}
Yellow LGT with natural faces	0.95–13.8 μm	0.76–14.2 μm	0.54–14.85 μm
Black LGT after repolishing	3.84–12.96 μm	3.20–13.55 μm	2.06–14.10 μm

(515 nm) at room temperature (300 K) and increases to 2.65 eV at 80 K. It substantially exceeds the band-gap value known for the isostructural silver tellurite AgGaTe$_2$ (1.316 eV) [5].

The intense absorption band centered near 16 μm determines the mid-IR transparency limit of LGT. It correlates with the two-phonon energy of the vibrational modes
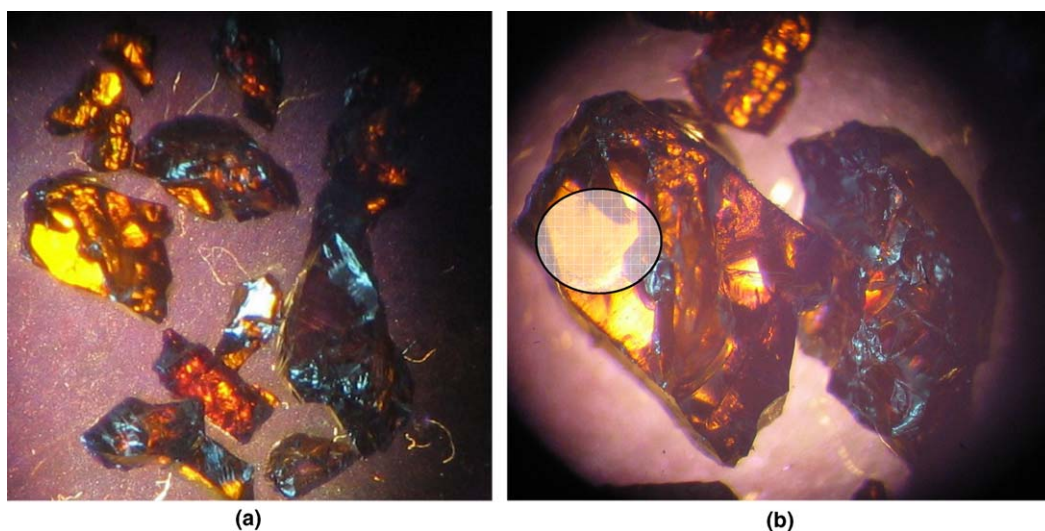
Fig. 1. As grown or cleaved pieces of LGT with natural faces of complicated form (a) The large piece in (b) with a clear face of about 1 mm^2 (shaded area) and optical path of about 1.7 mm was used for absorption measurements.
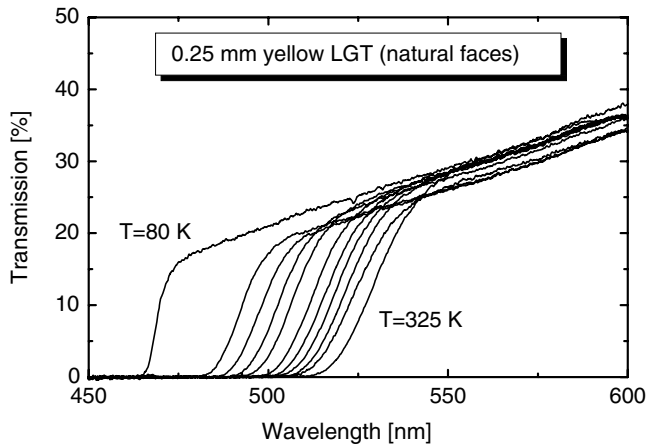
Fig. 3. Unpolarized transmission of a 0.25 mm thick plate of yellow as grown LGT with natural faces near the band-gap for temperatures (from left to right) $T = 80$, 170, 200, 220, 235, 255, 265, 276, 288, 300, and 325 K.

centered near 300 cm^{-1} which are observed in the Raman and IR-spectra of LGT [4].

3. Birefringence, dispersion, and non-linearity of LGT

The axial distortion ratio $(1 - c/2a = 7.7\%)$ is rather large in LGT. For an $A^I B^{III} C_2^{VI}$ chalcopyrite this ratio is a measure of the uniaxial tetragonal distortion from the underlying diamond-like face-centered cubic structure. Having in mind that $1 - c/2a = 9.2\%$ for AgGaSe$_2$ and 10.5% for AgGaS$_2$, it could be expected that LGT also possesses sufficient birefringence for phase-matching.

Measurement of the two refractive indices by the minimum deviation technique [4] indicated that $n_e > n_o$, hence LGT is a positive uniaxial crystal like ZnGeP$_2$ and AgGaTe$_2$, all three of them having the same point group $\bar{4}2\,m$. In contrast to AgGaTe$_2$ [5,6], however, the birefringence of LGT ($n_e - n_o \approx 0.1$) is indeed sufficient for phase-matching. The refractive indices of LGT can be fitted by the following Sellmeier equations valid in the 0.8–10 μm range:

$$n_o^2 = 6.24921 + 0.42592/(\lambda^2 - 0.0531) - 0.00149\lambda^2, \quad (1a)$$

$$n_e^2 = 6.70825 + 0.5667/(\lambda^2 - 0.01964) - 0.001\lambda^2, \quad (1b)$$

where λ is measured in μm. In accordance with its point group the effective non-linearity of LGT, when Kleinman symmetry holds, is given by:

$$d_{eeo} = d_{36} \sin 2\theta \cos 2\varphi, \quad (2a)$$

$$d_{oeo} = d_{eoo} = d_{36} \sin \theta \sin 2\varphi, \quad (2b)$$

for type-I and type-II phase-matching, respectively. Since LGT is a positive crystal the effective non-linearity is vanishing in the uncritical limit ($\theta = 90°$) for type-I phase-matching but this angle is anyway never reached for second-harmonic generation (SHG) within the transparency window.

The calculated phase-matching contours for non-degenerate three-wave interactions in LGT are shown in Fig. 4. Two branches of the solution can be seen in Fig. 4(a) for type-I (ee-o) phase-matching because the closed contours are interrupted at the transparency limits. With decreasing phase-matching angle the contours get smaller and degenerate into a point at about $\theta = 24.2°$. The transparency range of LGT can be covered for different λ_3 by varying θ roughly from 24° to 34° and hence d_{eff} is almost constant. The degenerate points correspond to SHG. The curves for type-II (oe-o and eo-o) phase-matching in Fig. 4(b) have a completely different shape. The two branches of the solution are represented by curves of opposite curvature that can cross at two points corresponding to degeneracy (SHG). With decreasing phase-matching angle these branches separate and a single crossing point is reached. For yet smaller phase-
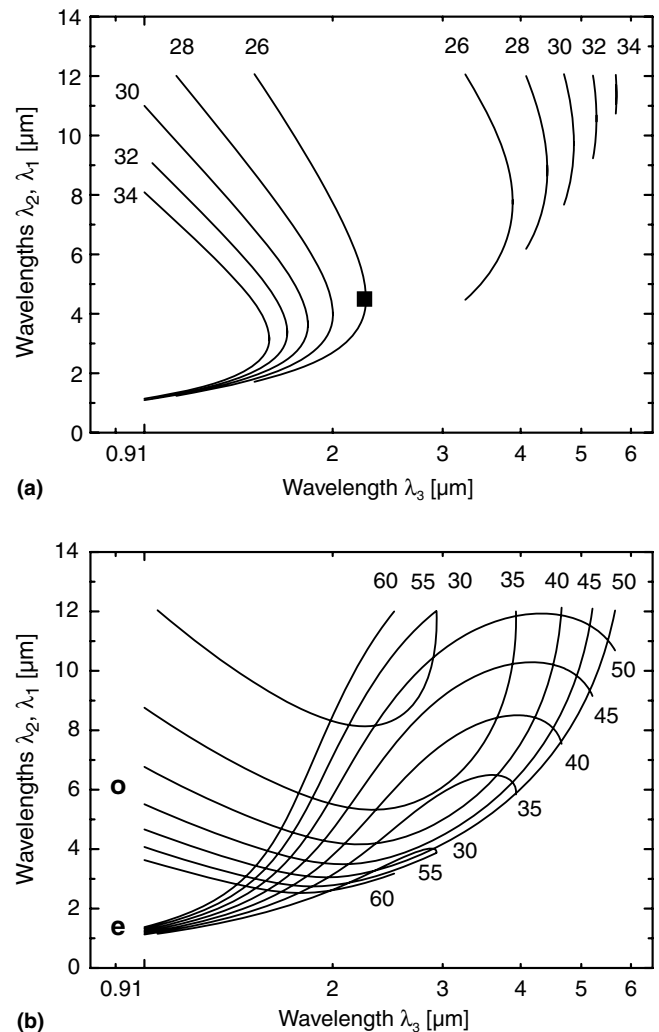

(a)

(b)

Fig. 4. Calculated three-wave interactions in LGT: (a) type-I (ee-o) phase-matching curves, and (b) type-II (oeo and eoo) phase-matching curves for several values of the polar angle θ indicated in the figures. The experimental point measured at $\lambda = 4.5$ μm is included as a square in (a). The curves are terminated by the transparency limits of the crystal. $1/\lambda_1 + 1/\lambda_2 = 1/\lambda_3$ holds.

Table 2
Chalcopyrite crystals of the $A^{I}B^{III}C_2^{VI}$ and $A^{II}B^{IV}C_2^{V}$ types and defect chalcopyrites of the $A^{II}B_2^{III}C_4^{VI}$ type for the non-linear optics

	E_g [eV]	n	$c/2a$	$n_e - n_o$	d_{36} [pm/V]	T [µm]	d_{36}^2/n^3 [pm^2/V^2]	d_{eff}^2/n^3 [pm^2/V^2]
AgGaS$_2$	2.76	2.37	0.895	−0.054	11.4	0.5–13.2	9.76	8.47
AgGaSe$_2$	1.83	2.60	0.908	−0.033	33.0	0.78–18	62.0	42.1
AgGaTe$_2$	1.32	2.98	0.953	0.016	70.1[a]	1.4–21	186[a]	NA
LiGaTe$_2$	2.41	2.54	0.923	0.094	39.3	0.95–13.8	94.3	74.6
ZnGeP$_2$	1.99	3.13	0.981	0.038	68.9	0.7–12.3	155	17.8[b]
CdGeAs$_2$	0.57	3.58	0.944	0.090	155.1	2.3–17.8	524	432
HgGa$_2$S$_4$	2.84	2.40	0.935	−0.041	20.5	0.59–12.8	30.4	NA

The refractive indices and the birefringence are estimated at 5.3 µm, and d_{36} and d_{eff} are evaluated for the 10.6–5.3 µm type-I SHG process.
E_g: direct band-gap, n: average refractive index, $c/2a$: tetragonal distortion, d_{36}: non-linear coefficient, T: transparency at a level of 3 cm^{-1}, d_{36}^2/n^3 and d_{eff}^2/n^3: figures of merit, NA: not applicable (no phase-matching).
[a] Theoretical estimations based on relative band-gap values.
[b] ZnGeP$_2$ seems to be phase-matchable at 10.6 µm depending on the supplier.

matching angles, no crossing point exists, and the degeneracy is not reached – see case $\theta = 35°$ in Fig. 4(b).

We estimated the non-linear coefficient d_{36} of LGT by comparing the SHG conversion efficiency at 4.5 µm to that obtained with ZnGeP$_2$ (both crystals type-I), using 250 fs pulses of 2 µJ energy generated by a KNbO$_3$ parametric amplifier operating at 1 kHz. Both samples were uncoated and 2 mm thick. Taking into account the different refractive indices, Fresnel reflections, absorption losses of LGT at the fundamental and second harmonic, and d_{36}(ZGP) = 75 pm/V [7], we arrived at d_{36}(LGT) = 43 pm/V ± 10%. The experimental angle was in excellent agreement (<0.2°) with the calculated one. Thus LGT is a highly non-linear optical crystal whose non-linear coefficient is much larger than for the related orthorhombic LiGaS$_2$ and LiGaSe$_2$ crystals (7 and 4.5 times, respectively), see [8].

Nowadays the chalcopyrites are the most widely used birefringent non-linear mid-IR crystals. From the remaining mid-IR crystals (CdSe, GaSe, Tl$_3$AsSe$_3$, Ag$_3$AsS$_3$, Ag$_3$SbS$_3$, LiInS$_2$, LiInSe$_2$, LiGaS$_2$, LiGaSe$_2$, etc.,) there are only few exceptions for which some real applications have been found. A summary of the relevant linear and non-linear optical properties of the chalcopyrite compounds belonging to the $A^{I}B^{III}C_2^{VI}$ and $A^{II}B^{IV}C_2^{V}$ families including the related defect chalcopyrites of the $A^{II}B_2^{III}C_4^{VI}$ type (point group $\bar{4}$) which are interesting for non-linear optics and in particular for SHG at 10.6 µm is given in Table 2. For comparison all the data available are reduced to 10.6 µm using Miller's rule for the non-linear polarizability. Some of the data in Table 2 is based on theoretical estimations. Note that of these crystals only AgGaS$_2$, AgGaSe$_2$ and ZnGeP$_2$ are commercially available and widely used while CdGeAs$_2$ and HgGa$_2$S$_4$ can be only obtained from some research laboratories. The birefringence of AgGaTe$_2$ which is included only for completeness is slightly too low for phase-matching and it was only suggested that solid solutions of the type AgGa(Se$_{1-x}$Te$_x$)$_2$, with non-linearity exceeding that of AgGaSe$_2$, might be useful [5]. Thus the compound LiGaTe$_2$ is the third chalcopyrite of the $A^{I}B^{III}C_2^{VI}$ type for which a phase-matched non-linear optical process has been demonstrated. At the same time it should be outlined that LGT exhibits the largest birefringence and highest non-linearity and figure of merit (d_{36}^2/n^3) as compared to AgGaS$_2$ and AgGaSe$_2$ (Table 2).

From Table 2 it can be seen that LGT holds a promise for CO$_2$ laser doubling at 10.6 µm, too. The figure of merit (last column) is higher than in AgGaS$_2$ and AgGaSe$_2$. We note that while the phase-matchability of ZnGeP$_2$ for SHG at 10.6 µm is still a subject of debate [9], both ZnGeP$_2$ and the highly non-linear CdGeAs$_2$ have additional problems: ZnGeP$_2$ exhibits at 10.6 µm already two-phonon absorption while the residual absorption of CdGeAs$_2$ at 5.3 cm is larger than 0.5 cm^{-1} and this crystal requires cryogenic cooling [10].

4. Conclusion

In conclusion, we demonstrated that the newly synthesized ternary semiconductor LGT belonging to the chalcopyrite class is a promising material for non-linear optical applications in the mid-IR. In particular LGT is transparent and phase-matchable for frequency doubling of CO$_2$ laser radiation at 10.6 µm possessing a very high figure of merit. Future studies will be devoted to the thermo-mechanical and thermo-optical properties of LGT, improvement of the crystal transmission and polishing techniques, and development of appropriate protective coatings.

References

[1] J. Brückner, 'I-III-VI-Verbindungshalbleiter mit Lithium als Gruppe I-Element: Kristallzüchtung und Charakterisierung', Dissertation, Albert-Ludwigs-Universität, Freiburg i. Br., Germany, 1997.
[2] L. Isaenko, A. Yelisseyev, S. Lobanov, A. Titov, V. Petrov, J.-J. Zondy, P. Krinitsin, A. Merkulov, V. Vedenyapin, J. Smirnova, Cryst. Res. Technol. 38 (2003) 379.
[3] L. Isaenko, I. Vasilyeva, A. Merkulov, A. Yelisseyev, S. Lobanov, J. Cryst. Growth 275 (2005) 217.

[4] L. Isaenko, P. Krinitsin, V. Vedenyapin, A. Yelisseyev, A. Merkulov, J.-J. Zondy, V. Petrov, Cryst. Growth Des 5 (2005) 1325.

[5] M.C. Ohmer, J.T. Goldstein, D.E. Zelmon, A.W. Saxler, S.M. Hedge, J.D. Wolf, P.G. Schunemann, T.M. Pollak, J. Appl. Phys. 86 (1999) 94.

[6] P.G. Shunemann, S.D. Setzler, T.M. Pollak, M.C. Ohmer, J.T. Goldstein, D.E. Zelmon, J. Cryst. Growth 211 (2000) 242.

[7] V. Petrov, F. Rotermund, F. Noack, P. Schunemann, Opt. Lett. 24 (1999) 414.

[8] V. Petrov, A. Yelisseyev, L. Isaenko, S. Lobanov, A. Titov, J.-J. Zondy, Appl. Phys. B 78 (2004) 543.

[9] K. Kato, Appl. Opt. 36 (1997) 2506.

[10] P.G. Schunemann, T.M. Pollak, MRS Bull. 23 (7) (1998) 23.